

Production of $\Lambda(1520)$

Seung-II Nam,^{1,2,*} Atsushi Hosaka,^{1,†} and Hyun-Chul Kim^{2,‡}

¹*Research Center for Nuclear Physics (RCNP),
Osaka University, Ibaraki, Osaka 567-0047, Japan*

²*Department of Physics and Nuclear Physics & Radiation Technology Institute (NuRI),
Pusan National University, Keum-Jung gu, Busan 609-735, Republic of Korea*

Abstract

We investigate the $\Lambda(1520)$ photoproduction via the reaction process, $\gamma N \rightarrow K\Lambda(1520)$. We employ the Born approximation and the Rarita-Schwinger formalism is used for $\Lambda(1520)$. We reproduce the total cross sections and the various angular distributions qualitatively well for the proton target and estimate them for the neutron one. We find that the contact term contributes much more to the process than the other kinematical channels. Taking into account this fact, we reanalyze the K^* -exchange dominance hypothesis suggested by the previous experiments.

PACS numbers: 13.75.Cs, 14.20.-c

Keywords: $\Lambda(1520)$, spin 3/2, photoproduction

arXiv:hep-ph/0505005v1 30 Apr 2005

*Electronic address: sinam@rcnp.osaka-u.ac.jp

†Electronic address: hosaka@rcnp.osaka-u.ac.jp

‡Electronic address: hchkim@pusan.ac.kr

I. INTRODUCTION

The observation of the evidence of the exotic pentaquark baryon Θ^+ has been one of the hottest issues in recent years in hadron physics [1]. However, there have been also many negative opinions and results for that evidence. Recently, the LEPS collaboration reported a new positive result for the evidence of the Θ^+ baryon from the deuteron target [2]. Interestingly, the production of Θ^+ took place together with $\Lambda(1520) (\equiv \Lambda^*)$ production. Therefore, it is natural to expect that there is a deep correlation between the productions of the two baryons, and it can be possible to extract information for the Θ^+ baryon by analyzing Λ^* instead.

At present, there are several experiments related to the photoproduction (A. Boyarski *et al.* [3] and D. P. Barber *et al.* [4]) and the electroproduction (S. P. Barrow *et al.* [5]) of Λ^* . It was reported that the photoproduction of Λ^* from the proton target was dominated by vector K^* -exchange by analyzing the Λ^* decay in the t -channel helicity frame [4]. On the other hand, it was claimed that the pseudoscalar K -exchange was the dominant contribution in the electroproduction [5].

In the present report, we investigate the Λ^* photoproduction via the reaction process $\gamma N \rightarrow K \Lambda^*$. As a frame work, we make use of the Born approximation which is expected to work properly in the low energy region. The Rarita-Schwinger vector-spinor formalism is introduced to treat spin-3/2 baryon (Λ^*) relativistically. A phenomenologically parameterized form factor is taken into account in gauge invariant manner.

We obtain qualitatively well reproduced total cross sections and momentum transfer t -dependence for the proton target case ($\gamma p \rightarrow K^+ \Lambda^*$) and estimate them for the neutron one ($\gamma n \rightarrow K^0 \Lambda^*$). The contact term contribution is found to be the most dominant contribution among various kinematical channels. This fact leads to the large difference in the order of magnitudes of the total cross sections for the proton and neutron targets ($\sigma_p \gg \sigma_n$). Vector K^* -exchange plays an important role to produce a characteristic angular distribution for the neutron target case. The K^* -exchange dominance hypothesis in the Λ^* photoproduction from the proton target [4] is reanalyzed by decomposing final spin state of the reaction. We observe that though spin(helicity)-3/2 final state is important as concluded by the previous analysis [4], the contribution of the spin-3/2 comes not only from the K^* -exchange but also from the contact term. Furthermore, we show the contribution from the contact term is larger than that from the K^* -exchange.

The present report will be organized as follows. In section 2 we will present the formalism for the present reaction calculations. section 3 will provide numerical results including total and differential cross sections and the t -dependence for the proton and neutron targets. A reanalysis of the K^* -exchange dominance hypothesis will be given in section 4. Finally, we will summarize our results and make a brief conclusion in section 5.

II. FORMALISM

We begin with the effective Lagrangians relevant to the $\gamma N \rightarrow K \Lambda^*$ process depicted in Fig. 1. We define the momenta of photon, pseudo-scalar kaon, vector kaon, nucleon and Λ^* as shown in the figure. For convenience, the vector K^* -exchange in the t -channel and contact diagrams will be called as the v -channel (vector channel) and c -channel (contact term channel), respectively. We need to consider all diagrams shown in Fig. 1 for the proton target, whereas only the magnetic (tensor) term of the s -channel, the K^* -exchange (v -

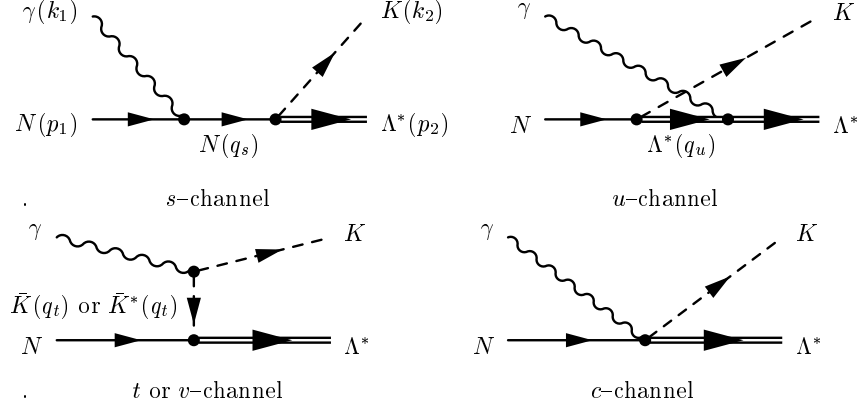


FIG. 1: The Feynmann diagrams

channel) and the u -channel are necessary for the neutron target due to charge neutrality. In order to formulate the effective Lagrangians including spin-3/2 particles, we employ the Rarita-Schwinger (RS) field formalism which we summarize in the Appendix.

The relevant effective Lagrangians are given as :

$$\begin{aligned}
\mathcal{L}_{\gamma NN} &= -e\bar{p} \left(\gamma_\mu + i \frac{\kappa_p}{2M_p} \sigma_{\mu\nu} k_1^\nu \right) A^\mu N + \text{h.c.}, \\
\mathcal{L}_{\gamma KK} &= ie \left\{ (\partial^\mu K^\dagger) K - (\partial^\mu K) K^\dagger \right\} A_\mu, \\
\mathcal{L}_{\gamma \Lambda^* \Lambda^*} &= -\bar{\Lambda}^{*\mu} \left\{ \left(-F_1 \not{\epsilon} g_{\mu\nu} + F_3 \not{\epsilon} \frac{k_{1\mu} k_{1\nu}}{2M_{\Lambda^*}^2} \right) - \frac{\not{k}_1 \not{\epsilon}}{2M_{\Lambda^*}} \left(-F_2 g_{\mu\nu} + F_4 \frac{k_{1\mu} k_{1\nu}}{2M_{\Lambda^*}^2} \right) \right\} \Lambda^{*\nu} \\
&+ \text{h.c.}, \\
\mathcal{L}_{\gamma KK^*} &= g_{\gamma KK^*} \epsilon_{\mu\nu\sigma\rho} (\partial^\mu A^\nu) (\partial^\sigma K) K^{*\rho} + \text{h.c.}, \\
\mathcal{L}_{K N \Lambda^*} &= \frac{g_{KN\Lambda^*}}{M_K} \bar{\Lambda}^{*\mu} \Theta_{\mu\nu}(A, Z) (\partial^\nu K) \gamma_5 p + \text{h.c.}, \\
\mathcal{L}_{K^* N \Lambda^*} &= -\frac{i g_{K^* N \Lambda^*}}{M_V} \bar{\Lambda}^{*\mu} \gamma^\nu (\partial_\mu K_\nu^* - \partial_\nu K_\mu^*) p + \text{h.c.}, \\
\mathcal{L}_{\gamma K N \Lambda^*} &= -i \frac{e g_{KN\Lambda^*}}{M_K} \bar{\Lambda}^{*\mu} A_\mu K \gamma_5 N + \text{h.c.}, \tag{1}
\end{aligned}$$

where N , Λ_μ^* , K and A^μ are the nucleon, Λ^* , pseudoscalar kaon and photon fields, respectively. The interaction for $K^* N \Lambda^*$ vertex is taken from Ref. [14]. As for the $\gamma \Lambda^* \Lambda^*$ vertex for the u -channel, we utilize the effective interaction suggested by Ref. [15] which contains four form factors of different multipoles. We ignore the electric coupling F_1 , since Λ^* is neutral. We also neglect F_3 and F_4 terms, assuming that higher multipole terms are less important. Hence, for the photon coupling to Λ^* , we consider only the magnetic coupling term F_2 whose strength is proportional to the anomalous magnetic moment of Λ^* , κ_{Λ^*} which is treated as a free parameter. The off-shell term $\Theta_{\mu\nu}(A, Z)$ of a general spin-3/2 particle is defined as follows [12, 13] :

$$\Theta_{\mu\nu}(A, Z) = g_{\mu\nu} + \left\{ \frac{1}{2} (1 + 4Z) A + Z \right\} \gamma_\mu \gamma_\nu. \tag{2}$$

If we choose $A = -1$ [7, 12, 13], we can rewrite Eq. (2) in the following form with new parameter $X = -(Z + 1/2)$:

$$\Theta_{\mu\nu}(X) = g_{\mu\nu} + X\gamma_\mu\gamma_\nu. \quad (3)$$

Here, we will regard X as a free parameter in the present work.

In order to determine the coupling constant $g_{KN\Lambda^*}$, we make use of the full width $\Gamma_{\Lambda^*} = 15.6$ MeV and the branching ratio 0.45 for the decay $\Lambda^* \rightarrow \bar{K}N$ [16]. The coupling constant $KN\Lambda^*$ can be obtained by the following relation :

$$g_{KN\Lambda^*} = \left\{ \frac{P_3}{4\pi M_{\Lambda^*}^2 M_K^2 \Gamma_{\Lambda^*}} \left(\frac{1}{4} \sum_{\text{spin}} |\mathcal{M}'|^2 \right) \right\}^{-\frac{1}{2}}, \quad i\mathcal{M}' = \bar{u}(P_2)\gamma_5 P_3^\mu u_\mu(P_1), \quad (4)$$

where P_1 , P_2 and P_3 are the momenta of Λ^* , N and \bar{K} , respectively for the two body decay $\Lambda^* \rightarrow \bar{K}N$ in the center of mass frame. Thus, we obtain $g_{KN\Lambda^*} \sim 11$. As for the $K^*N\Lambda^*$ coupling constant, we will choose the values of $|g_{K^*N\Lambda^*}| = 0$ and $|g_{KN\Lambda^*}| = 11$ for the numerical calculation. In the non-relativistic quark model, if Λ^* is described as a p -wave excitation of flavor-singlet spin-3/2 state, it is shown that the strength of the $K^*N\Lambda^*$ coupling constant is of the same order as that of $KN\Lambda^*$ or even larger than that. The coupling constant of $g_{\gamma K^*K}$ is taken to be 0.254 [GeV $^{-1}$] for the charged decay and 0.388 [GeV $^{-1}$] for the neutral decay [16].

Taking all of these into consideration, we construct the invariant amplitudes as follows :

$$\begin{aligned} i\mathcal{M}_s &= -\frac{eg_{KN\Lambda^*}}{M_K} \bar{u}^\mu(p_2, s_2) k_{2\mu} \gamma_5 \frac{(\not{p}_1 + M_p)F_c + \not{k}_1 F_s}{q_s^2 - M_p^2} \not{e} u(p_1, s_1), \\ &+ \frac{e\kappa_p f_{KN\Lambda^*}}{2M_p M_K} \bar{u}^\mu(p_2, s_2) k_{2\mu} \gamma_5 \frac{(\not{q}_s + M_p)F_s}{q_s^2 - M_p^2} \not{e} \not{k}_1 u(p_1, s_1) \\ i\mathcal{M}_u &= -\frac{f_{KN\Lambda^*} \kappa_{\Lambda^*}}{2M_K M_\Lambda} \bar{u}_\mu(p_2) \not{k}_1 \not{e} D_\sigma^\mu \Theta^{\sigma\rho} k_{2\rho} \gamma_5 u(p_1) F_u, \\ \mathcal{M}_t &= \frac{2ef_{KN\Lambda^*}}{M_K} \bar{u}^\mu(p_2, s_2) \frac{q_{t,\mu} k_2 \cdot \epsilon}{q_t^2 - M_K^2} \gamma_5 u(p_1, s_1) F_c, \\ i\mathcal{M}_c &= \frac{ef_{KN\Lambda^*}}{M_K} \bar{u}^\mu(p_2, s_2) \epsilon_\mu \gamma_5 u(p_1, s_1) F_c, \\ i\mathcal{M}_v &= \frac{-ig_{\gamma K^*K} g_{K^*NB}}{M_{K^*} (q_t^2 - M_K^2)} \bar{u}^\mu(p_2, s_2) \gamma_\nu (q_t^\mu g^{\nu\sigma} - g_t^\nu q^{\mu\sigma}) \epsilon_{\rho\eta\xi\sigma} k_1^\rho \epsilon^\eta k_2^\xi u(p_1, s_1) F_v, \end{aligned} \quad (5)$$

where u^μ is the RS vector-spinor which is defined as follows :

$$u^\mu(p_2, s_2) = \sum_{\lambda, s} \left(1\lambda \frac{1}{2} s \middle| \frac{3}{2} s_2 \right) e^\mu(p_2, \lambda) u(p_2, s), \quad (6)$$

with the Clebsh-Gordon coefficient $(1\lambda \frac{1}{2} s \middle| \frac{3}{2} s_2)$. $D_{\mu\nu}$ stands for the spin-3/2 propagator :

$$D_{\mu\nu} = -\frac{\not{q} + M_{\Lambda^*}}{q^2 - M_{\Lambda^*}^2} \left\{ g_{\mu\nu} - \frac{1}{3} \gamma_\mu \gamma_\nu - \frac{2}{3M_{\Lambda^*}^2} q_\mu q_\nu + \frac{q_\mu \gamma_\nu + q_\nu \gamma_\mu}{3M_{\Lambda^*}} \right\}. \quad (7)$$

In Eq. (5), we have shown how the four-dimensional form factor is inserted in such way that gauge-invariance is preserved. As suggested in Ref. [17, 18], we adopt the following parameterization for the four-dimensional gauge- and Lorentz-invariant form factor:

$$F_x(q^2) = \frac{\Lambda^4}{\Lambda^4 + (x - M_x^2)^2}, \quad x = s, t, u, v$$

$$F_c = F_s + F_t - F_s F_t. \quad (8)$$

The form of F_c is chosen such that the on-shell values of the coupling constants are reproduced. The cutoff masses, Λ will be determined to produce the $\gamma p \rightarrow K^+ \Lambda^*$ total cross section data.

III. NUMERICAL RESULTS

A. $\gamma N \rightarrow K \Lambda^*$ without the form factors

In this subsection, we present the numerical results for the $\gamma N \rightarrow K \Lambda^*$ without the form factors in order to see the bare contributions from each channel. In the upper two panels of

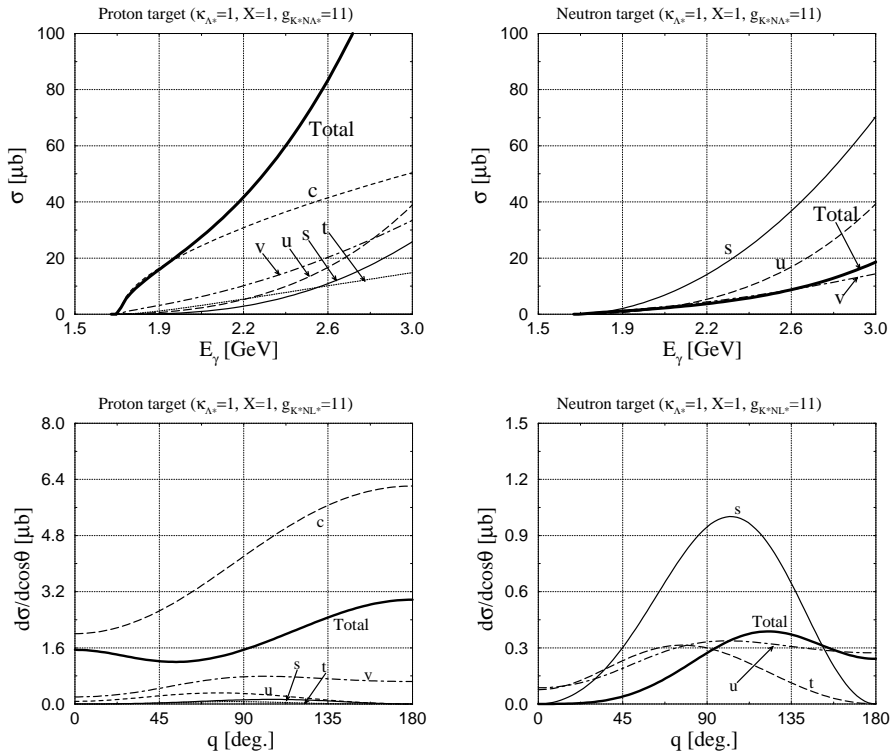


FIG. 2: Various contributions to the total cross (upper two panels) and differential (lower two panels) sections for the proton target (left panel) and the neutron target (right panel) without a form factor. The differential cross sections are obtained for $E_\gamma = 2.0$ GeV. We choose the unknown parameters $(\kappa_{\Lambda^*}, X) = (1, 1)$ and the coupling constant $g_{K N \Lambda^*} = +11$.

Fig. 2, we present various contributions to the total cross sections for the proton and neutron

targets without form factors. Here, we fix the unknown parameters $\kappa_{\Lambda^*} = 1.0$, $X = 1$ and $g_{K^*N\Lambda^*} = g_{KN\Lambda^*} = +11$. Later, we discuss parameter dependence of our calculation. In the case of the proton target in the left panel of Fig. 2, we observe that the contribution of the contact term (c -channel) is dominant over other channels. We also note that the c - and v -channels demonstrate the s -wave threshold behavior ($\sigma \sim (E_\gamma - E_{\text{th}})^{1/2}$), where E_{th} stands for the threshold energy, although the magnitude of the v -channel is smaller than that of the c -channel. However, the other channels, s , u and t start with p -wave contribution in the vicinity of the threshold. This kinematical effect explains why the s -, u - and t -channels are relatively suppressed especially near the threshold region as compared with the c - and v -channels containing the s -wave contribution. For the neutron target (right panel), the s -channel is the dominant contribution, because we have no neutral charge coupling in the c -channel. We also find destructive interference between the s -, u - and v -channels. We also show the differential cross sections in the upper two panels of Fig. 2 without the form factor. The differential cross sections are obtained for $E_\gamma = 2.0$ GeV.

B. $\gamma N \rightarrow K\Lambda^*$ with the form factor

In this subsection, we present the numerical results for the Λ^* photoproduction with the form factor given in Eq. (8). The experimental data are taken from Ref. [4] In Fig. 3, we

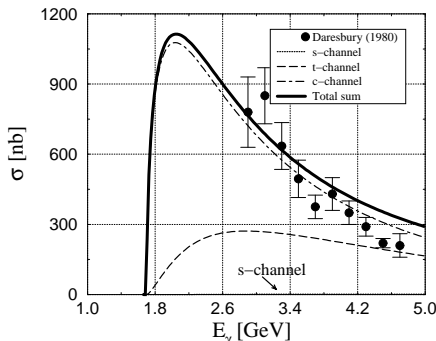


FIG. 3: The total cross sections for the proton target with the form factor. We show the s -, t - and c -channels, separately. The contribution of the s -channel is negligibly small.

show the total cross sections including s -, t - and c -channels which do not contain unknown parameters κ_{Λ^*} , X and $g_{K^*N\Lambda^*}$. The experimental data are taken from Ref. [4] with photon energies in the range of $2.8 \text{ GeV} < E_\gamma < 4.8 \text{ GeV}$. In the present calculation, we have chosen the cutoff parameter $\Lambda = 700 \text{ MeV}$, which can reproduce the experimental data very well from the threshold to the higher energy region. However, the results in the higher energy region should not be taken seriously since the Born approximation works properly in the low energy region near the threshold. In fact, we have verified that the total cross sections depend much on the parameters, κ_{Λ^*} and X , beyond $E_\gamma \gtrsim 3 \text{ GeV}$, whereas the parameter dependence is rather weak for $E_\gamma \lesssim 3 \text{ GeV}$ [19]. Therefore, we focus most of our discussion below the energy region $E_\gamma \lesssim 3 \text{ GeV}$, where the Born approximation of the effective Lagrangian method is expected to work. It is interesting to observe that the size

and energy dependence of the total cross section of the $\Lambda^*(1520)$ production are similar to those of the production of the ground state $\Lambda(1116)$ [3, 4].

In Fig. 3, we have also shown separate contributions from the s -, t - and c -channels. Obviously, the c -channels contribution dominates, which is the important feature of the reaction with the proton. In order to see the role of K^* -exchange, we consider the two cases $g_{K^*N\Lambda^*} = \pm|g_{K^*N\Lambda^*}|$ and compare the results to the case without the $K^*N\Lambda^*$ coupling, i.e. $g_{K^*N\Lambda^*} = 0$. In Fig. 4, we compare the total cross sections up to $E_\gamma \lesssim 3$ GeV using

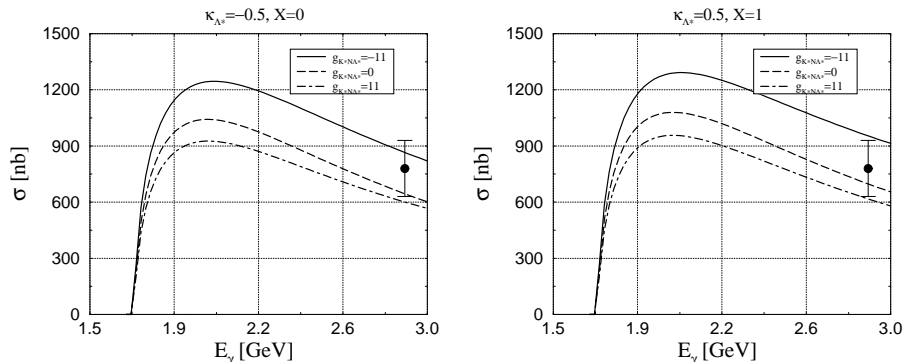


FIG. 4: The total cross sections for the proton target with the form factor. We choose $(\kappa_{\Lambda^*}, X) = (-0.5, 0)$ and $(0.5, 1)$ in order to see the parameter dependence. We choose three different values of the coupling constant $g_{K^*N\Lambda^*} = 0$ and ± 11 .

the different $K^*N\Lambda^*$ coupling strengths. The total cross sections are rather insensitive to the contribution of K^* -exchange, a consequence that the c -channel contribution is still dominant for the proton target.

These two results are compared for the two different parameter sets, $(\kappa_{\Lambda^*}, X) = (-0.5, 0)$ and $(0.5, 1)$. As discussed previously, the results do not depend much on these parameters at low-energies $E_\gamma \lesssim 3$ GeV. In the quark model, it is found that the anomalous magnetic moment κ_{Λ^*} turns out to vanish in the $SU(3)$ limit for a pure flavor singlet Λ^* . Taking into account that the effect of explicit $SU(3)$ symmetry breaking, we expect that the values of κ_{Λ^*} may lie in the range of $|\kappa_{\Lambda^*}| < 0.5$. However, from Fig. 4, we expect that the dependence on κ_{Λ^*} within this range is small. Therefore, these two parameters κ_{Λ^*} and X can be set zero, i.e. $\kappa_{\Lambda^*} = X = 0$.

In Fig. 5, we plot the dependence on the momentum transfer, $d\sigma/dt$ (t -dependence) at $E_\gamma = 3.8$ GeV which is the average energy of the Daresbury experiment ($2.8 < E_\gamma < 4.8$ GeV) [4]. The figure indicates good agreement with the data. In Fig. 6, we also demonstrate the angular dependence. Here, θ is the angle between the incident photon and the outgoing kaon in the center of mass system. Each panel draws the differential cross sections $d\sigma/d(\cos\theta)$ with $g_{K^*N\Lambda^*}$ varied. We observe that K^* -exchange does not contribute much to the differential cross sections as in the case of the total cross sections (see Fig. 4).

Now, we discuss the case of the neutron target. In this case, the c -channel contribution vanishes, and therefore, the total cross section becomes much smaller than the case of the proton target especially when the form factor is employed. The left panel of Fig. 7 shows the total cross sections with and without K^* -exchange. When K^* -exchange is switched off, only the s -channel plays a role. Furthermore, in the neutron target case, the p -wave contribution is dominant, which leads to the energy dependence $(E_\gamma - E_{\text{th}})^{3/2}$ of the total

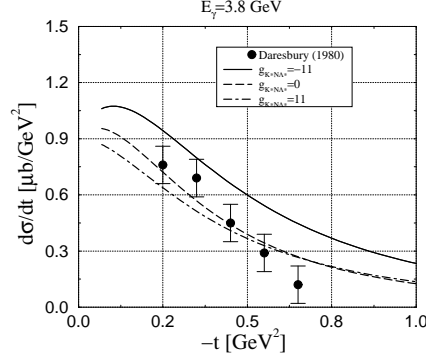


FIG. 5: The t -dependence for the proton target at $E_\gamma = 3.8$ GeV. We choose $(\kappa_{\Lambda^*}, X) = (0, 0)$.

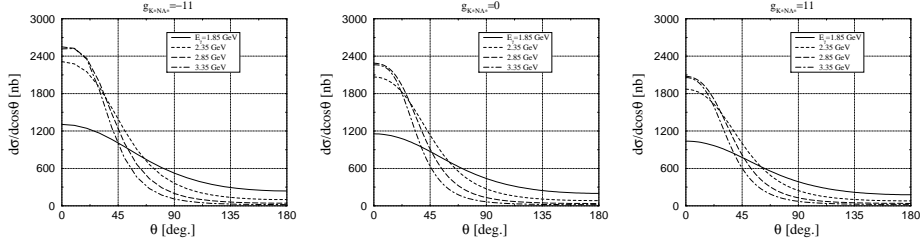


FIG. 6: The differential cross sections for the proton target with the form factor. Several photon energies are taken into account. We choose $(\kappa_{\Lambda^*}, X) = (0, 0)$.

cross sections as clearly indicated in Fig. 7. The inclusion of K^* -exchange enhances the total cross sections with the energy dependence $\sim (E_\gamma - E_{\text{th}})^{1/2}$. The contribution of K^* -exchange is important for the neutron target. However, the magnitude of that contribution is still small as compared to the proton target. Experimental study of the energy dependence will be useful to obtain the informations of the reaction mechanism.

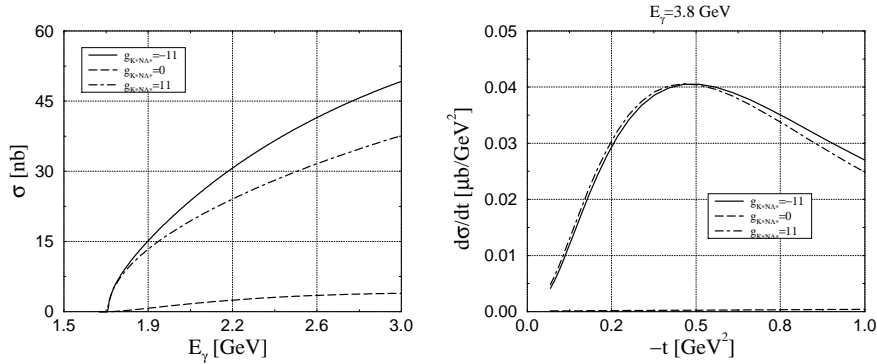


FIG. 7: The left panel : the total cross sections for the neutron target with the form factor. We use $(\kappa_{\Lambda^*}, X) = (0, 0)$. We choose three different values of the coupling constants $g_{K^*N\Lambda^*} = 0$ and ± 11 . The right panel : the t -dependence for the neutron target with the form factor at $E_\gamma = 3.8$ GeV.

Turning to the t -dependence, we demonstrate it in the right panel of Fig. 7, where we

choose once again $E_\gamma = 3.8$ GeV. The t -dependence of the neutron target is very much different from the proton one, since the relevant diagrams are different.

In Fig. 8, we show the angular dependence for the neutron target, using the form factor. With the K^* -exchange being included, the differential cross sections are enhanced around $\sim 45^\circ$. Note that the sign of $g_{K^*N\Lambda^*}$ is not important. The bump around 45° is a typical behavior coming from the K^* -exchange.

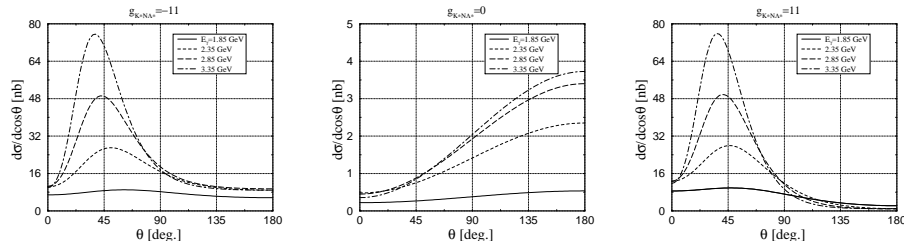


FIG. 8: The differential cross sections for the neutron target with the form factor. Several photon energies are taken into account. We choose $(\kappa_{\Lambda^*}, X) = (0, 0)$.

IV. THE ROLE OF K^* -EXCHANGE

In Ref. [4] of the Daresbury experiment, it was argued that the Λ^* photoproduction was dominated by vector K^* -exchange (v -channel) rather than pseudoscalar K -exchange (t -channel) by analyzing the decay amplitude in the t -channel in the helicity basis of the Λ^* . If the helicity of the Λ^* is $S_z = \pm 3/2$, the decay of $\Lambda^* \rightarrow K^- p$ is explained by $\sin^2 \theta$ in which θ is the angle between the two kaons in the helicity basis (see Ref. [5] for details). On the other hand, the angular dependence becomes $1/3 + \cos^2 \theta$ for the decay of the $S_z = \pm 1/2$ state. Therefore, taking into account the ratio of these two helicity amplitudes, one could extract information which meson would dominate. In Ref. [4], it was shown that the ratio of $(S_z = \pm 1)/(S_z = \pm 3/2)$ was nearly zero. Thus, it was suggested that the Λ^* photoproduction was dominated by the v -channel.

In Fig. 9, we plot the t -dependence for each helicity using the form factor with three different values for the coupling constants $g_{K^*N\Lambda^*}$. We choose $E_\gamma = 3.8$ GeV as done previously. In Fig. 9, we observe that the $S_z = \pm 3/2$ contribution is dominant especially in

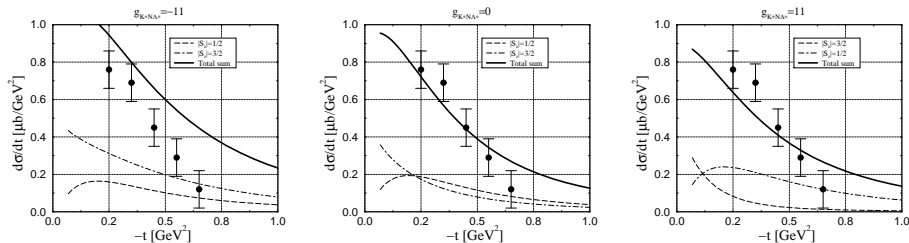


FIG. 9: The t -dependence for each helicity of the Λ^* in the final state. We change the coupling constant $g_{K^*N\Lambda^*}$. We choose $(\kappa_{\Lambda^*}, X) = (0, 0)$.

the region $-t \lesssim 0.2 \text{ GeV}^{-2}$. There is also a small contribution from the $S_z = \pm 1/2$. However,

we find that even without the v -channel ($g_{K^*N\Lambda^*} = 0$), the $S_z = \pm 3/2$ does not become zero. Therefore, the $S_z = \pm 3/2$ contribution comes from not only the v -channel but also from the other channels.

In order to see this situation more carefully, we pick up three important channels, the c -, t - and v -channels, and plot the t -dependence for each helicity in Fig. 10. One can see that the $S_z = \pm 1/2$ contribution is larger than that of the $S_z = \pm 3/2$ for the pseudoscalar K -exchange (t -channel), and vice versa for the v -channel. We also observe that the c -channel has sizable contributions to both $S_z = \pm 1/2$ and $S_z = \pm 3/2$ amplitudes.

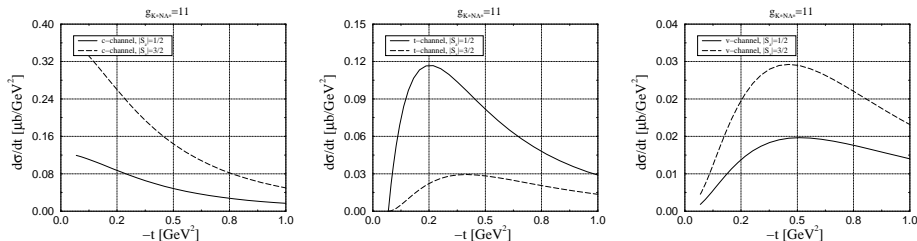


FIG. 10: The t -dependence for the two helicities $S_z = \pm 1/2$ and $S_z = \pm 3/2$ for the c -, t - and v -channels.

From these observations, our diagram calculation indicates that the $S_z = \pm 3/2$ contribution is significant as shown in Ref [4]. However, most of the $S_z = \pm 3/2$ contribution comes from the c -channel, not from the v -channel as suggested in Ref. [4]. We also find that the sizable $S_z = \pm 1/2$ contributions are produced from the c - and t -channels. Therefore, in order to reproduce a nearly zero value of the ratio of $(S_z = \pm 1/2)/(S_z = \pm 3/2)$ [4], we need a more suppression factor in the t -channel, which is the major source of the $S_z = \pm 1/2$ contribution in the Λ^* photoproduction.

V. SUMMARY AND CONCLUSION

In the present work, we investigated the $\Lambda^*(1520, 3/2^-)$ photoproduction via the $\gamma N \rightarrow K\Lambda^*$ reaction. We employed the Rarita-Schwinger formalism for describing the spin-3/2 particle for a relativistic description. Using the effective Lagrangians for the Born diagrams, we constructed the invariant amplitudes for the reaction. We have investigated carefully the dependence on the model parameters including various meson-baryon coupling constants and form factors. Numerical results were then presented using reasonable sets of the parameters for relatively low energy region $E_\gamma \lesssim 3$ GeV. Important results are then summarized in Table. I where the features of the $\gamma p \rightarrow K^+\Lambda^*$ and $\gamma n \rightarrow K^0\Lambda^*$ are shown. Turning to the

Reactions	$\gamma p \rightarrow K^+\Lambda^*$	$\gamma n \rightarrow K^0\Lambda^*$
σ	~ 900 nb	~ 30 nb
$d\sigma/d(\cos \theta)$	Forward peak	Bump at $\sim 45^\circ$
$d\sigma/dt$	Good	No data

TABLE I: Summary of the results.

helicity dependence, though the contribution of the $S_z = \pm 3/2$ was dominant, it was not

directly related to the K^* -exchange dominance as indicated in the previous experimental analysis. We hope that the present work will provide a guideline to understanding the structure and reactions for $\Lambda(1520)$.

Acknowledgments

We thank T. Nakano, H. Toki, A. Titov, E. Oset and M. J. Vicente Vacas for fruitful discussions and comments. The work of S.I.N. has been supported by the scholarship from the Ministry of Education, Culture, Science and Technology of Japan. The works of A.H. and S.I.N. are partially supported by the collaboration program of RCNP, Osaka Univ., Japan and IFIC, Valencia Univ., Spain. The work of A.H. is also supported in part by the Grant for Scientific Research ((C) No.16540252) from the Education, Culture, Science and Technology of Japan. The works of H.C.K. and S.I.N. are supported by the Korean Research Foundation (KRF-2003-070-C00015).

Appendix

A. Rarita-Schwinger vector-spinor

We can write the RS vector-spinors according to their spin states as follows:

$$\begin{aligned}
u^\mu(p_2, \frac{3}{2}) &= e_+^\mu(p_2)u(p_2, \frac{1}{2}), \\
u^\mu(p_2, \frac{1}{2}) &= \sqrt{\frac{2}{3}}e_0^\mu(p_2)u(p_2, \frac{1}{2}) + \sqrt{\frac{1}{3}}e_+^\mu(p_2)u(p_2, -\frac{1}{2}), \\
u^\mu(p_2, -\frac{1}{2}) &= \sqrt{\frac{1}{3}}e_-^\mu(p_2)u(p_2, \frac{1}{2}) + \sqrt{\frac{2}{3}}e_0^\mu(p_2)u(p_2, -\frac{1}{2}), \\
u^\mu(p_2, -\frac{3}{2}) &= e_-^\mu(p_2)u(p_2, -\frac{1}{2}).
\end{aligned} \tag{9}$$

Here, we employ the basis four-vectors, e_λ^μ which are written by

$$\begin{aligned}
e_\lambda^\mu(p_2) &= \left(\frac{\hat{e}_\lambda \cdot \vec{p}_2}{M_B}, \quad \hat{e}_\lambda + \frac{\vec{p}_2(\hat{e}_\lambda \cdot \vec{p}_2)}{M_B(p_2^0 + M_B)} \right) \text{ with} \\
\hat{e}_+ &= -\frac{1}{\sqrt{2}}(1, i, 0), \quad \hat{e}_0 = (0, 0, 1) \quad \text{and} \quad \hat{e}_- = \frac{1}{\sqrt{2}}(1, -i, 0).
\end{aligned} \tag{10}$$

[1] T. Nakano *et al.* [LEPS Collaboration], Phys. Rev. Lett. **91**, 012002 (2003); V. V. Barmin *et al.* [DIANA Collaboration], Phys. Atom. Nucl. **66**, 1715 (2003) [Yad. Fiz. **66**, 1763 (2003)]; S. Stepanyan *et al.* [CLAS Collaboration], Phys. Rev. Lett. **91**, 252001 (2003); V. Kubarovsky *et al.* [CLAS Collaboration], Erratum-ibid. **92**, 049902 (2004) [Phys. Rev. Lett. **92**, 032001

- (2004)]; J. Barth *et al.* [SAPHIR Collaboration], hep-ex/0307083; A. Airapetian *et al.* [HERMES Collaboration], Phys. Lett. B **585**, 213 (2004).
- [2] T. Nakano, talks in the international workshop Chiral 05, RIKEN and in the Japna-US workshop 2005, Osaka Univ.. February (2005).
- [3] A. Boyarski, R. E. Diebold, S. D. Ecklund, G. E. Fischer, Y. Murata, B. Richter and M. Sands, Phys. Lett. B **34**, 547 (1971).
- [4] D. P. Barber *et al.*, Z. Phys. C **7**, 17 (1980).
- [5] S. P. Barrow *et al.* [Clas Collaboration], Phys. Rev. C **64**, 044601 (2001).
- [6] W. Rarita and J. S. Schwinger, Phys. Rev. **60**, 61 (1941).
- [7] B. J. Read, Nucl. Phys. B **52**, 565 (1973).
- [8] K. Johnson and E. C. G. Sudarshan, Annals Phys. **13**, 126 (1961).
- [9] G. Velo and D. Zwanziger, Phys. Rev. **188**, 2218, (1969).
- [10] V. Pascalutsa, Phys. Rev. D **58**, 096002 (1998).
- [11] G. Hoehler, H. P. Jakob and R. Strauss, Nucl. Phys. B **39**, 237(1972).
- [12] L. M. Nath, B. Etemadi and J. D. Kimel, Phys. Rev. D **3**, 2153, (1971).
- [13] C. R. Hagen, Phys. Rev. D **4**, 2204 (1971).
- [14] R. Machleidt, K. Holinde and C. Elster, Phys. Rept. **149**, 1 (1987).
- [15] M. Gourdin, Nuovo Cimento 36, 129 (1965); and, 40A, 225 (1965).
- [16] S. Eidelman *et al.* [Particle Data Group], Phys. Lett. B **592**, 1 (2004).
- [17] R. M. Davidson and R. Workman, arXiv:nucl-th/0101066.
- [18] H. Haberzettl, C. Bennhold, T. Mart and T. Feuster, Phys. Rev. C **58**, 40 (1998).
- [19] S. I. Nam, A. Hosaka and H. -Ch. Kim, talk in the few-body workshop at RCNP (2004), hep-ph/0502143.
- [20] S. I. Nam, A. Hosaka and H. -Ch. Kim, Phys. Lett. B **579**, 43 (2004).
- [21] S. I. Nam, A. Hosaka and H. -Ch. Kim, arXiv:hep-ph/0403009.
- [22] F. E. Close and J. J. Dudek, Phys. Lett. B **586**, 75 (2004).